

Simulation of Three-Stage Nylon 6 Reactors with Intermediate Mass Transfer at Finite Rates

SANTOSH K. GUPTA,* ANIL KUMAR, and K. K. AGRAWAL,
*Department of Chemical Engineering, Indian Institute of Technology,
Kanpur-208016, India*

Synopsis

A three-stage isothermal nylon 6 reactor with a kinetic scheme incorporating ring opening, polycondensation, polyaddition, cyclic dimer formation, and reaction with monofunctional acids has been modeled. In the first and third stages, removal of the condensation by-product, water, is prevented. The second stage of this sequence, however, involves finite rates of diffusion of water to cocurrently flowing inert gas bubbles. The number-average chain length of the polymer obtained in this reactor differs substantially from that obtained assuming instantaneous water removal and is a function of the various design variables. It is observed that several choices of these design variables can be made to obtain the same product, thus emphasizing the need for more comprehensive optimization studies than hitherto carried out.

INTRODUCTION

Nylon 6 is a polymer having considerable commercial significance and is produced by water-initiated polymerization of ϵ -caprolactam. Recently, there has been a spurt in activity in the area of simulation and optimization of industrial nylon 6 reactors. Reimschuessel et al.¹⁻⁴ considered the following three major reversible reactions: (a) ring opening reaction, in which the ring of the monomer, ϵ -caprolactam, is opened by water molecules to form aminocaproic acid; (b) polycondensation reaction in which the amino and carboxylic acid end groups react to form large polymer chains via amide linkages, with water formed as a condensation product; (c) polyaddition reaction in which monomer adds on to the growing polymer chains. They obtained the monomer conversion and the number-average chain length λ_n of the polymer produced for different feed conditions. Their experimental results over an extended range of temperatures were found to be consistent with earlier work of Hermans et al.^{5,6} Kruissink et al.,⁷ and Wiloth.^{8,9}

Later, Tirrell et al.¹⁰ incorporated the reaction with monofunctional acids (modifiers) in their kinetic scheme and, in addition to the conversion and the number-average chain length, also obtained the second moment of the chain length distribution. Mochizuki and Ito^{11,12} subsequently incorporated the formation of macrocyclic compounds in the reaction scheme and simulated and optimized the nylon 6 reactor. Their optimal temperature and water concentration profiles compared favorably with those obtained by Naudin ten Cate,¹³ who used a different objective function. Tai and co-workers¹⁴⁻¹⁷ have recently obtained accurate experimental data and have curve-fitted their results to obtain a better set of rate constants for nylon 6 polymerization. They used their data to simulate various commonly used industrial reactors.¹⁸

* To whom correspondence should be addressed.

Gupta et al.¹⁹⁻²¹ obtained the entire molecular weight distribution (MWD) for various isothermal polymerizations by solving the mass balance equations numerically. They used two kinetic models for the formation of macrocyclic compounds based on the work of Jacobson and Stockmayer²² and Andrews et al.²³ and studied their effect on the MWDs. Similar MWDs were later obtained by these workers²⁴ for polymerization in homogeneous, continuous flow, stirred-tank reactors with removal of water. Gupta and Gandhi²⁵ recently used a combination of direct numerical integration of mass balance equations and Laguerre polynomials to obtain the molecular weight distributions more efficiently.

Though some attempts have been made to model real reactors, most simulation studies have been restricted in scope in view of the fact that they are limited to isothermal batch polymerizations with either no water removal or instantaneous intermediate water removal.^{1,10,11,13,26} Both of these are mathematical idealizations. Optimization studies^{1,12,13,26} that have been carried out demonstrate clearly that a high water concentration must be maintained initially in order to achieve high monomer conversion, whereas a low water concentration should exist later on so that polymer of high molecular weight is obtained through the condensation step. Indeed, the VK tube⁴ has been reported to accomplish this combination admirably.

Jacobs and Schweigman²⁷ discuss other patented reactors in which the vaporization of water is prevented in the initial stage (stage I) of polymerization by maintaining high pressures. The water is then removed by flashing (stage II) before carrying out the polymerization in the third stage with no water removal. Based on the simplicity of the VK column, they mention a new scheme of polymerization in which the feed is pumped at sufficiently high pressure with water removal in the intermediate stage by bubbling an inert gas as shown in Figure 1. The simulation of such polymerization reactors has not been accomplished till now for want of appropriate models accounting for finite rates of water removal. In this report, an attempt has been made to bridge this gap. In addition, the equations developed herein can be used to give more meaningful optimization results.

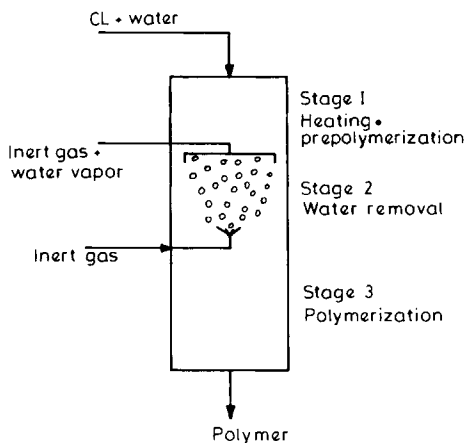


Fig. 1. A typical three-stage nylon 6 reactor with removal of water in stage II using inert gas.

FORMULATION

The kinetic scheme used in this study is given in Table I, in which the rate constants are those corresponding to the reaction between functional groups (as defined by Flory²⁹). Appropriate weighting factors must be used with these in writing mass balance equations for molecular species, as discussed in our earlier simulation work on reversible ARB polymerizations characterized by unequal reactivity of functional groups.^{30,31} It may be mentioned that the kinetic scheme given in Table I is a slight improvement over our previous publication²⁰ in that the more recent information on cyclic dimer formation and the corresponding polyaddition step¹⁶ has been used. Because of this change, the mass balance equations for the various species are slightly different from those of Table II of Ref. 20.

The forward rate constants k_i ($i = 1, 2, \dots, 5$) are expressed in terms of the acid end-group concentration (in g-mol/kg mixture) as

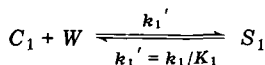
$$k_i = k_i^0 + k_i^c \sum_{n=1}^{\infty} ([A_n] + [S_n]) \equiv k_i^0 + k_i^c (\mu_0 + \mu'_0) \tag{1}$$

with k_i , k_i^0 , and k_i^c having units of kg/mol-hr and kg²/mol²-h, respectively. k_i^0 and k_i^c are, in turn, given by an Arrhenius-type relation as follows:

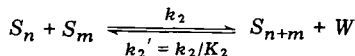
$$\log k = \log A^* - \frac{E \text{ (cal/mol)}}{4.574T \text{ (K)}} \tag{2}$$

TABLE I
Kinetic Scheme for Nylon-6 Polymerization^a

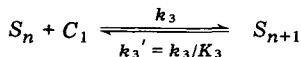
1. Ring Opening:



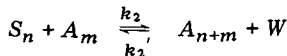
2. Polycondensation:



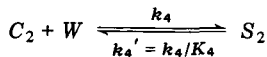
3. Polyaddition:



4. Reaction with Monofunctional Acid:



5. Ring Opening of Cyclic Dimer:

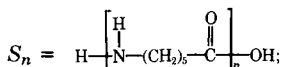


6. Polyaddition of Cyclic Dimer:



^a $C_1 = \epsilon$ -caprolactam; $C_2 = \text{H}-\text{N}-(\text{CH}_2)_5-\overset{\text{O}}{\parallel}\text{C}-\text{N}(\text{H})-\text{CH}_2-\overset{\text{O}}{\parallel}\text{C}$

W = water;



and $A_n = \text{X}-\left[\overset{\text{O}}{\parallel}\text{C}-\text{N}(\text{H})-(\text{CH}_2)_5 \right]_{n-1}-\overset{\text{O}}{\parallel}\text{C}-\text{OH}$, where X is unreactive group.

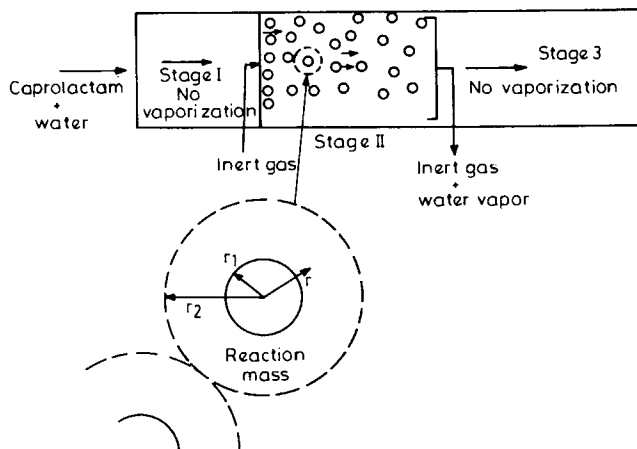


Fig. 2. Model for cocurrent water removal in stage II.

The equilibrium constants K_i are similarly given as a function of temperature:

$$\log K_i = \frac{\Delta S_i \text{ (e.u.)}}{4.574} - \frac{\Delta H_i \text{ (cal/mol)}}{4.574T \text{ (K)}} \quad (3)$$

Values of A^* , E , ΔS_i , and ΔH_i for the various reactions have been given by Arai et al.¹⁶

Mass balance (continuity) equations are now written for stage II of the polymerization reactor wherein water is removed at a finite rate by means of bubbles of inert gas, as in Figure 1. However, in order to keep the analysis simple and yet obtain a first-order approximation to the effect of finite mass transfer rates on nylon 6 polymerization, it is assumed that the gas bubbles move in the same direction (cocurrently) as the reaction mass, as shown in Figure 2. With the gas bubbles "floating" along with the reaction mass, one may associate a certain sphere of influence for each gas bubble. In general, these spheres will be of different sizes, depending on the diameter of the spherical gas bubbles and the spacing between neighboring bubbles. However, since these are random variables, one can, on an average, represent stage II as shown in the inset of Figure 2, with r_1 being the average radius of the gas bubbles and r_2 half of the average center-to-center distance between neighboring bubbles. Both r_1 and r_2 , in general, would depend on the physical properties of the reaction mass as well as the shape of the sparger, but these have been treated as parameters in this study. A similar model for the mass transfer of condensation product has been studied earlier for ARB polycondensations characterized by unequal reactivity of functional groups.^{32,33}

For nylon 6 polymerization, the mass balance equations are given in Table II, where D_w is the diffusivity of water, W , through the polymeric reaction mass and μ_k and μ'_k are the moments of linear bifunctional and monofunctional compounds:

$$\begin{aligned} \mu_k &\equiv \sum_{n=1}^{\infty} n^k [S_n] \\ \mu'_k &\equiv \sum_{n=1}^{\infty} n^k [A_n] \quad k = 0, 1, 2, 3 \end{aligned} \quad (4)$$

In writing these equations, the following assumptions have been made:

(1) Only the condensation product W can diffuse. The monomeric and polymeric species do not diffuse at all. The concentration of W in the reaction mass is small and there is no mixing (convective) effect in the reaction mass. Similar approximations have been made by Secor³⁴ and Amon and Denson³⁵ earlier. Only in the study of Reimschuessel et al.³⁶ has this approximation been relaxed where the diffusion of monomer along with W has been considered. It was shown that the diffusion of the former is small because of its low concentration and diffusivity.

TABLE II
Mass Balance Equations for System of Figure 2

$$\begin{aligned} \frac{\partial \mu_0}{\partial t} &= k_1[C_1][W] - k'_1[S_1] - k_2\mu_0^2 + k'_2[W](\mu_1 - \mu_0) \\ &\quad - k_2\mu_0\mu'_0 + k'_2[W](\mu'_1 - \mu'_0) + k_4[W][C_2] - k'_4[S_2] \\ \frac{\partial \mu'_0}{\partial t} &= 0 \\ \frac{\partial \mu_1}{\partial t} &= k_1[C_1][W] - k'_1[S_1] + k_3[C_1]\mu_0 - k'_3(\mu_0 - [S_1]) - k_2\mu_0\mu_1 - k'_2[W]\left(\frac{\mu_1 - \mu'_2}{2}\right) + 2k_5[C_2]\mu_0 \\ &\quad - 2k'_5(\mu_0 - [S_1] - [S_2]) + 2k_4[W][C_2] - 2k'_4[S_2] \\ \frac{\partial \mu'_1}{\partial t} &= k_2\mu_1\mu'_0 - \frac{k'_2[W]}{2}(\mu'_2 - \mu'_1) \\ \frac{\partial \mu_2}{\partial t} &= k_1[C_1][W] - k'_1[S_1] + 2k_2\mu_1^2 + \frac{k'_2}{3}[W](\mu_1 - \mu_3) + k_3[C_1](\mu_0 + 2\mu_1) \\ &\quad + k'_3(\mu_0 - 2\mu_1 + [S_1]) - k_2\mu_2\mu'_0 + \frac{k'_2}{6}[W](2\mu'_3 - 3\mu'_2 + \mu'_1) + 4k_5[C_2](\mu_1 + \mu_0) \\ &\quad + 4k'_5(\mu_0 - [S_1] - [S_2]) - 4k'_5(\mu_1 - [S_1] - 2[S_2]) + 4k_4[W][C_2] - 4k'_4[S_2] \\ \frac{\partial \mu'_2}{\partial t} &= k_2(2\mu_1\mu'_1 + \mu_2\mu'_0) - \frac{k'_2[W]}{6}(4\mu'_3 - 3\mu'_2 - \mu'_1) \\ \frac{\partial [C_1]}{\partial t} &= -k_1[C_1][W] + k'_1[S_1] - k_3[C_1]\mu_0 + k'_3(\mu_0 - [S_1]) \\ \frac{\partial [S_1]}{\partial t} &= k_1[C_1][W] - k'_1[S_1] - 2k_2[S_1]\mu_0 + 2k'_2[W](\mu_0 - [S_1]) - k_3[S_1][C_1] \\ &\quad + k'_3[S_2] - k_2\mu'_0[S_1] + k'_2[W](\mu'_0 - [A_1]) - k_5[S_1][C_2] + k'_5[S_3] \\ \frac{\partial [A_1]}{\partial t} &= -k_2[A_1]\mu_0 + k'_2[W](\mu'_0 - [A_1]) \\ \frac{\partial [C_2]}{\partial t} &= -k_4[C_2][W] + k'_4[S_2] - k_5[C_2]\mu_0 + k'_5(\mu_0 - [S_1] - [S_2]) \\ \frac{\partial [W]}{\partial t} &= D_w \left\{ \frac{\partial^2 [W]}{\partial r^2} + \frac{2}{r} \frac{\partial [W]}{\partial r} \right\} - k_1[C_1][W] + k'_1[S_1] + k_2(\mu_0)^2 - k'_2[W](\mu_1 - \mu_0) \\ &\quad + k_2\mu_0\mu'_0 - k'_2[W](\mu'_1 - \mu'_0) - k_4[C_2][W] + k'_4[S_2] \end{aligned}$$

(2) The interfacial water concentration W_s at $r = r_1$ is taken to be constant and is treated as a parameter. W_s would, in general, depend upon the thermodynamic equilibrium relation existing between the gas phase and the reaction mass and would change with time. The assumption of W_s as constant would be valid only when the conditions existing in the reactor do not change considerably over the entire path of the gas bubble. This approximation is good when there are several small bubbles in the system.

(3) There is no resistance to mass transfer in the gas phase. This is expected to be small since the diffusivity of water through the relatively viscous reaction mass is much lower than its value through the gas phase. In the present study, however, this assumption is not required because of the choice of W_s as a parameter.

The equations for the moments $\mu_0, \mu_1, \mu_2, \mu'_0, \mu'_1,$ and μ'_2 have been obtained by using the z -transforms defined by

$$D(z,t) = \sum_{n=1}^{\infty} z^{-n} [S_n]$$

$$D^*(z,t) = \sum_{n=1}^{\infty} z^{-n} [A_n] \quad (5)$$

The differential equations governing the change of D and D^* are first obtained using exact expressions of $[S_n]$ and $[A_n]$. These are subsequently differentiated to obtain the various moments. This method is identical to that used by Tai et al.^{16,17} These moment equations were also verified by appropriate summations of the mass balance equations for S_n and A_n .

In order to solve the mass balance equations of Table II, it is required to "break" the hierarchy of equations. The following approximations are used for this purpose:

$$[S_1] = [S_2] = [S_3] \quad (6a)$$

$$\mu_3 = \frac{\mu_2(2\mu_2\mu_0 - \mu_1^2)}{\mu_1\mu_0} \quad (6b)$$

$$\mu'_3 = \frac{\mu'_2(2\mu'_2\mu'_0 - \mu'_1{}^2)}{\mu'_1\mu'_0} \quad (6c)$$

Equations 6(b) and 6(c) have been obtained assuming that the concentrations of the bifunctional and monofunctional molecules are well described by the Schultz-Zimm function at any time. These hierarchy-breaking approximations, again, have been found reasonable in earlier studies¹⁷ in the polymerization of nylon 6 in the absence of diffusion of W and without monofunctional compounds.

The set of equations in Table II are solved along with eq. (6) with $D_w = 0$ in the first stage of the three-stage reactor. Various initial values of $[W]_0$ and $[A_1]_0$ are used which are typically encountered in industrial practice. After the reaction is carried out for a certain time θ_1 in stage I, the material enters stage II where water diffuses toward the inert gas bubble. The initial and boundary conditions required for this stage are given by

$t = \theta_1, \quad r_1 < r \leq r_2$: all concentrations = output concentration of stage I

$$\theta_1 \leq t \leq \theta_2: \quad r = r_1 \quad [W] = W_s; \quad r = r_2 \quad \frac{\partial [W]}{\partial r} = 0 \text{ (symmetry)} \quad (7)$$

The spatial-average concentration of any species or moment μ_k or μ'_k in the second stage is obtained using an equation of the following type:

$$[\bar{C}_1] = \frac{3}{r_2^3 - r_1^3} \int_{r_1}^{r_2} [C_1] r^2 dr \quad (8)$$

The second stage is assumed to end where the spatial-average water concentration reaches a fixed fraction f of the value entering in that stage. Thereafter, the reaction mass enters the third stage where there is no diffusion of water. It is assumed that the outgoing stream of the second stage is instantaneously mixed before it enters the third stage.

The number- and weight-average chain lengths can be computed at any stage as follows:

$$\begin{aligned} \lambda_n &= \frac{\mu_1 + \mu'_1}{\mu_0 + \mu'_0} \\ \lambda_w &= \frac{\mu_2 + \mu'_2}{\mu_1 + \mu'_1} \end{aligned} \quad (9)$$

The polydispersity index ρ , is given by

$$\rho = \frac{\lambda_w}{\lambda_n} = \frac{(\mu_2 + \mu'_2)(\mu_0 + \mu'_0)}{(\mu_1 + \mu'_1)^2} \quad (10)$$

SIMULATION PROCEDURE

The explicit finite difference method, which is sometimes called the forward marching technique,³⁷ was used for solving the partial differential equations with a time increment Δt of $1/200$ h. The spatial increment Δr was fixed by using the equality condition of the following convergence criterion³⁷:

$$\frac{(\Delta r)^2}{(\Delta t)D_w} \geq 4 \quad (11)$$

Details of this procedure are also given in Ref. 33.

The program was checked by computing the total concentration of $-(\text{CH}_2)_5-$ groups $\{= 2[C_2] + \sum_{n=1}^{\infty} n[A_n] + [C_1] + \sum_{n=1}^{\infty} n[S_n]\}$ at any position and time and comparing it with the initial value $\{= [A_1]_0 + [C_1]_0 + [S_1]_0\}$. This check came out to within 0.0001% in the worst possible case. Such a check has been found to be an extremely sensitive one in our earlier studies.³⁰⁻³²

The integration of these equations took approximately 45 s on a DEC-1090 system to reach a polymerization time of about 20 h. Also, the results on monomer conversion and λ_n in the absence of diffusion of W matched well those of Reimschuessel et al.¹

RESULTS AND DISCUSSION

Several simulations of a nylon 6 reactor were carried out, both with and without removal of water. Figures 3-6 show the results in the absence of water removal for various situations given in Table III. On comparison of runs 1-4, it is observed that even though the conversion of caprolactam is almost insensitive to whether the rate constants of Reimschuessel et al.⁴ are used or those of Tai et

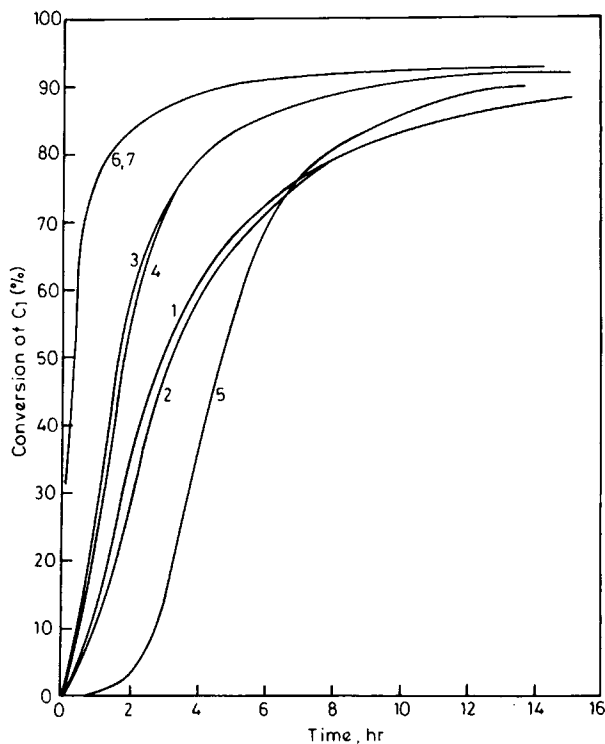


Fig. 3. Caprolactam conversion for the various simulation runs indicated in Table III.

al.,¹⁶ there is a discernible difference as far as λ_n and ρ are concerned. λ_n is lower when the rate constants of Tai et al. are used, while the value of ρ at large polymerization times is higher. Results on C_2 vs. time as obtained by the present model are almost indistinguishable from values obtained using the equations of Tai et al.,¹⁶ implying that the minor errors in their derivations do not influence the final results substantially.

A significant conclusion that was reached from a comparison of this study (run 3) using equations for moments with our previous results^{19,20} using direct integration of species equations was that in the presence of monofunctional acid stabilizers, the conversion, λ_n , and ρ were almost indistinguishable. In fact, at

TABLE III
Conditions Used for Simulation Runs Shown in Figures 3-6 (No Removal of Water)^a

Run no.	[W] ₀ , g-mol/kg mix	[A] ₁ ₀ , g-mol/kg mix	[S] ₁ ₀ , g-mol/kg mix	Cyclization	Rate constants of
1	0.22	0.088	0	No	Reimschuessel et al. ⁴
2	0.22	0.088	0	Yes, Tai et al. ¹⁶	Tai et al. ¹⁶
3	0.44	0.088	0	No	Reimschuessel et al. ⁴
4	0.44	0.088	0	Yes, Tai et al. ¹⁶	Tai et al. ¹⁶
5	0.44	0	0	Yes, Tai et al. ¹⁶	Tai et al. ¹⁶
6	0	0	0.44	Yes, Tai et al. ¹⁶	Tai et al. ¹⁶
7	0	0.088	0.44	Yes, Tai et al. ¹⁶	Tai et al. ¹⁶

^a $[C_1]_0 = 8.8$ g-mol/kg mix, $T = 235^\circ\text{C}$ for all runs.

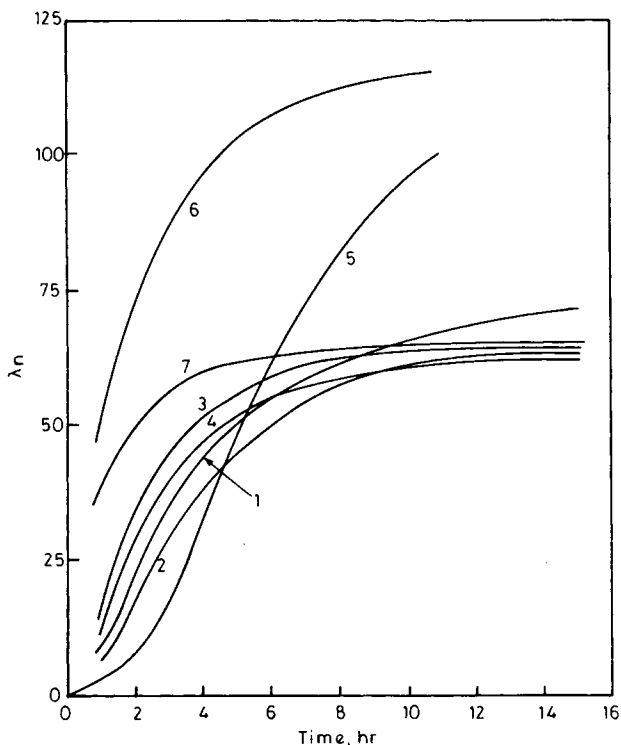


Fig. 4. Number-average chain length λ_n for various simulation runs indicated in Table III.

$t = 8$ h, μ'_0 , μ'_1 , and μ'_2 were 0.088, 5.414, and 702.944, respectively for run 3, while our earlier results gave corresponding values of 0.08796, 5.358, and 705.35, respectively. This implies that the use of the moment closure equation, 6(c), for

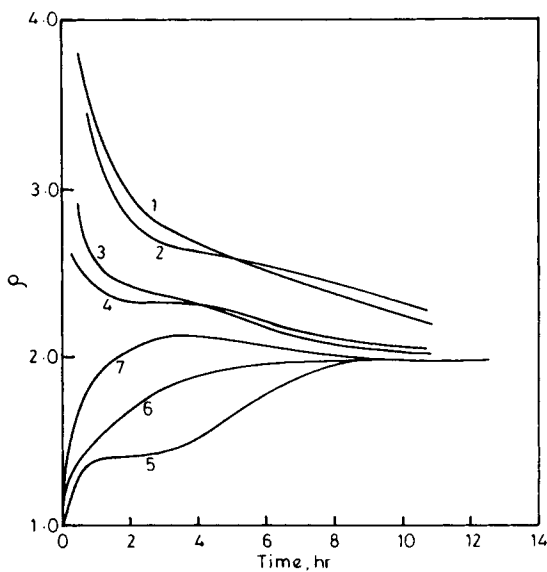


Fig. 5. Polydispersity index ρ for various simulation runs indicated in Table III.

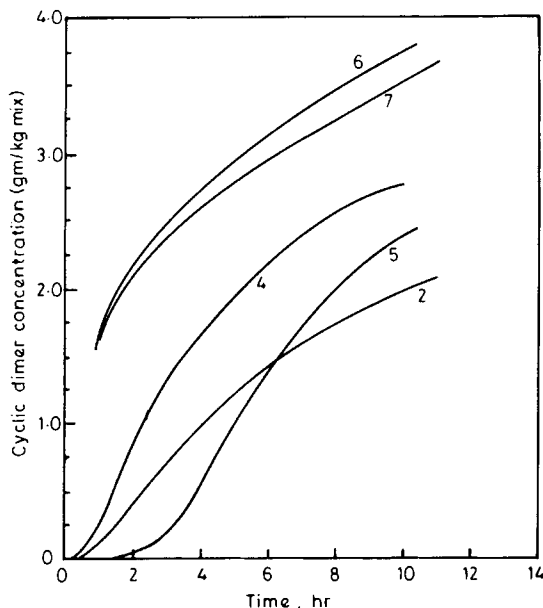


Fig. 6. Cyclic dimer concentrations in g/kg mix for various simulation runs indicated in Table III.

monofunctional molecules is justified. The effect of varying the initial concentrations of water, $[W]_0$, and of monofunctional acid, $[A_1]_0$, on the product properties is similar to that predicted by earlier studies. The conversion is speeded up by increasing $[W]_0$ and $[A_1]_0$ although the equilibrium value of λ_n decreases simultaneously. Figures 3–5 also indicate the effect of substituting water by aminocaproic acid (S_1) as the ring-opening agent (this may be obtained by depolymerizing scrap nylon 6 in a plant). The use of S_1 instead of W for ring opening was first reported by Kruissink et al.,⁷ and Gupta and Gandhi³⁸ have recently indicated its usefulness in reactor design. Both the monomer conversion as well as λ_n are substantially higher with S_1 replacing W , though larger amounts of cyclic compounds are formed. This suggests a change in the technology of nylon 6 production provided S_1 can be made available inexpensively. This also suggests that the use of a recycle stream containing S_1 from some point within the reactor may prove beneficial in reducing the residence time ($[S_1]$ shows a maximum at a point near the entrance, at $\theta \simeq 2$ h, and the recycle stream may be drawn from here). A feasibility study of such a scheme is in progress.³⁹

The effect of finite mass transfer rates of water removal in the three-stage reactor is shown in Figures 7 and 8 for different situations. Figure 7 shows the results at 265°C when the initial water concentration at the beginning of stage I is 0.0652 mol/mol caprolactam, and there are no monofunctional molecules. Stage I ends at $t = \theta_1 = 4.67$ h when λ_n is 83.8. In the absence of any water removal, λ_n attains a value of 84.1 as shown by curve A. In contrast, if *all* the water present at $t = \theta_1$ is removed *instantaneously*, and the reaction mass goes to stage III, λ_n increases to an equilibrium value of 234, as shown by curve B. This corresponds very closely to run III-1 of Reimschuessel and Nagasubramanian.¹ As mentioned above, such an instantaneous removal of water is not physically possible.

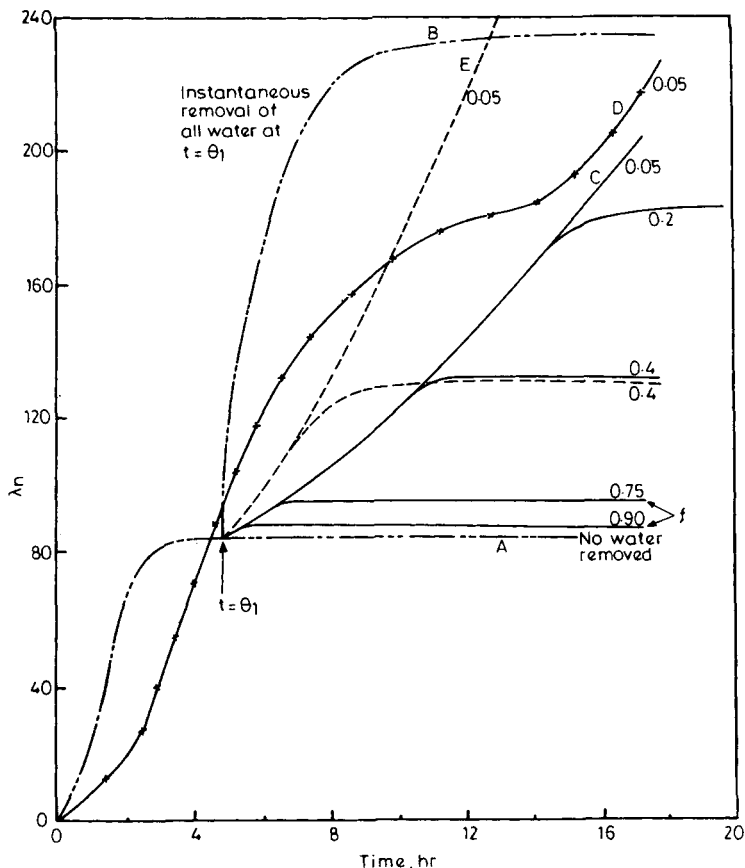


Fig. 7. Plot of λ_n vs. time in the reactor of Fig. 2. Solid lines are for larger sparse inert gas bubbles, while dotted lines are for smaller dense bubbles; (—X—) for $[W]_0 = 0.0155$ mol/mol caprolactam. For all other curves, $[W]_0 = 0.0652$ mol/mol caprolactam. Values of f indicated; $T = 265^\circ\text{C}$, $[A_1]_0 = 0$, $W_s = 0$ in stage II, $[S_1]_0 = 0$; (—) and (—X—) $r_1 = 3.79$ mm; $r_2 = 22.76$ mm; (---) $r_1 = 2.68$ mm, $r_2 = 16.10$ mm.

For the model shown in Figure 2, two runs have been made in order to get an idea of the effect of various parameters. In one case (shown by solid lines), inert bubbles of radii (r_1) 3.79 mm with center-to-center distance ($2r_2$) of 45.52 mm have been used to effect water removal. In the other case (shown by dotted lines), smaller and more closely spaced bubbles ($r_1 = 2.68$ mm, center-to-center spacing 32.2 mm) are used. The value of D_w is taken as 0.9×10^{-4} m²/h as reported by Nagasubramanian and Reimschuessel.³⁶ It may be mentioned that these values have been chosen somewhat arbitrarily, but they give a good idea of the range of numbers typically encountered. The interfacial water concentration W_s has been taken as zero, but no change has been observed by increasing W_s to 0.001 g-mol/g-mol caprolactam. Stage II ends when the spatial-average water concentration becomes f times the value at the beginning of stage II. It is observed from Figure 7 that the increase in λ_n in the third stage is not very significant—in fact, it is advantageous to conduct polymerization with continuous removal of water till the desired value of λ_n is obtained. In all these runs, it was observed that very little difference exists in the final monomer conversion and

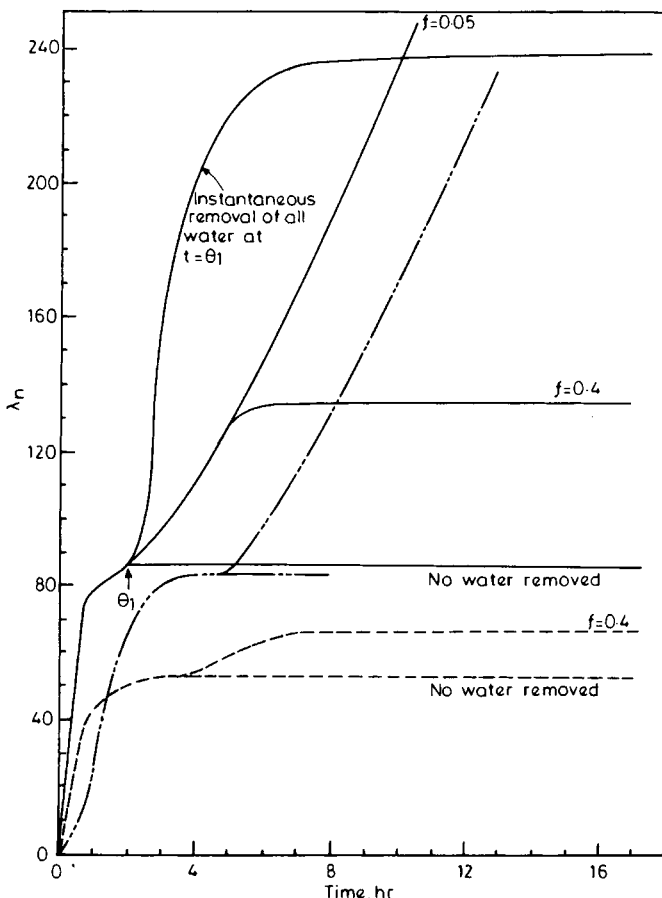


Fig. 8. Plot of λ_n vs. time in reactor of Fig. 2. Solid lines: $[W]_0 = 0$, $[S_1]_0 = 0.0652$ mol/mol caprolactam. $[A_1]_0 = 0$, $T = 265^\circ\text{C}$, $W_s = 0$ or 0.001 mol/mol caprolactam; dotted lines: $[W]_0 = 0.0652$ mol/mol caprolactam, $[A_1]_0 = 0.088$ mol/kg mix, $[S_1]_0 = 0$, $W_s = 0$, $T = 265^\circ\text{C}$; (---) curve E of Fig. 7; (—) and (---) $r_1 = 2.68$ mm, $r_2 = 16.10$ mm.

the polydispersity index. Thus, several routes exist to reach the same final results. For example: (a) a high initial water concentration may be used to get a high monomer conversion in a short time with relatively low λ_n in the first stage, followed by a continuous removal of water for a longer period of time in stage II, as in curve C; (b) a lower initial water concentration may be used to get the same monomer conversion in a longer time, followed by a shorter period in stage II, as in the case shown by curve D in Figure 7. A comparison of curves C and D suggests strongly the need for optimization studies using the costs of various operations in order to arrive at a set of optimal operating conditions.

Figure 8 shows similar results on the three-stage cocurrent reactor of Figure 2, with aminocaproic acid used instead of water for ring opening and with monofunctional acid present in the feed. It is apparent that even in the presence of mass transfer, ring opening by S_1 leads to the same product molecular weight in far shorter reactor lengths. The conversion of caprolactam and the polydispersity index are almost the same as in Figure 7.

References

1. H. K. Reimschuessel and K. Nagasubramanian, *Chem. Eng. Sci.*, **27**, 1119 (1972).
2. H. K. Reimschuessel and K. Nagasubramanian, *Polym. Eng. Sci.*, **12**, 179 (1972).
3. H. K. Reimschuessel, in *Ring Opening Polymerization*, 1st ed., K. C. Frisch and S. L. Reegen, Eds., Dekker, New York, 1969.
4. H. K. Reimschuessel, *J. Polym. Sci. Macromol. Rev.*, **12**, 65 (1977).
5. P. H. Hermans, D. Heikens, and P. F. Van Velden, *J. Polym. Sci.*, **30**, 81 (1958).
6. D. Heikens, P. H. Hermans, and G. M. Van der Want, *J. Polym. Sci.*, **44**, 437 (1960).
7. Ch. A. Kruissink, G. M. Vander Want, and A. Staverman, *J. Polym. Sci.*, **30**, 67 (1958).
8. F. Wiloth, *Makromol. Chem.*, **15**, 98 (1955).
9. F. Wiloth, *Makromol. Chem.*, **30**, 189 (1959).
10. M. V. Tirrell, G. H. Pearson, R. A. Weiss, and R. L. Laurence, *Polym. Eng. Sci.*, **15**, 386 (1975).
11. S. Mochizuki and N. Ito, *Chem. Eng. Sci.*, **28**, 1139 (1973).
12. S. Mochizuki and N. Ito, *Chem. Eng. Sci.*, **33**, 1401 (1978).
13. W. F. H. Naudin ten Cate, *Proc. Intern. Congr. Use of Elec. Comp. in Chem. Eng.*, Paris, April 1973.
14. K. Tai, H. Teranishi, Y. Arai, and T. Tagawa, *J. Appl. Polym. Sci.*, **24**, 211 (1979).
15. K. Tai, H. Teranishi, Y. Arai, and T. Tagawa, *J. Appl. Polym. Sci.*, **25**, 77 (1980).
16. Y. Arai, K. Tai, H. Teranishi, and T. Tagawa, *Polymer*, **22**, 273 (1981).
17. K. Tai, Y. Arai, H. Teranishi, and T. Tagawa, *J. Appl. Polym. Sci.*, **25**, 1789 (1980).
18. K. Tai, Y. Arai, and T. Tagawa, *J. Appl. Polym. Sci.*, **27**, 731 (1982).
19. S. K. Gupta, A. Kumar, P. Tandon, and C. D. Naik, *Polymer*, **22**, 481 (1981).
20. S. K. Gupta, C. D. Naik, P. Tandon, and A. Kumar, *J. Appl. Polym. Sci.*, **26**, 2153 (1981).
21. S. K. Gupta and A. Kumar, *Chem. Eng. Commun.*, to appear.
22. H. Jacobson and W. H. Stockmayer, *J. Chem. Phys.*, **18**, 1600 (1950).
23. J. M. Andrews, F. R. Jones, and J. A. Semlyen, *Polymer*, **15**, 420 (1974).
24. S. K. Gupta, A. Kumar, and A. Ramagopal, *Polym. Eng. Sci.*, to appear.
25. A. Gupta and K. S. Gandhi, *J. Appl. Polym. Sci.*, **27**, 1099 (1982).
26. P. J. Hoftyzer, J. Hoofschagen, and D. W. Van Krevelen, *Proc. 3rd Eur. Symp. Chem. Rxn. Eng.*, Amsterdam, Sept. 15-17, 1964.
27. J. Jacobs and C. Schweigman, *Proc. 5th Eur./2nd Intl. Symp. Chem. Rxn. Eng.*, Amsterdam, May 2-4, 1972.
28. To Vereinigte Glanzstoff Fabriken, Ger. Pat. 1.167.021 (1962).
29. P. J. Flory, *Principles of Polymer Chemistry*, 1st ed., Cornell University Press, Ithaca, N.Y., 1953.
30. A. Kumar, P. Rajora, N. L. Agrawalla, and S. K. Gupta, *Polymer*, **23**, 222 (1982).
31. S. K. Gupta, N. L. Agarwalla, P. Rajora, and A. Kumar, *J. Polym. Sci. Polym. Phys. Ed.*, to appear.
32. S. K. Gupta, N. L. Agarwalla, and A. Kumar, *J. Appl. Polym. Sci.*, **27**, 1217 (1982).
33. S. K. Gupta, A. Kumar, and K. K. Agrawal, *Polymer*, to appear.
34. R. M. Secor, *A.I.Ch.E.J.*, **15**, 861 (1969).
35. M. Amon and C. D. Denson, *Ind. Eng. Chem. Fundam.*, **19**, 415 (1980).
36. K. Nagasubramanian and H. K. Reimschuessel, *J. Appl. Polym. Sci.*, **17**, 1663 (1973).
37. W. H. Ray and J. Szekeley, *Process Optimization*, 1st ed., Wiley-Interscience, New York, 1973.
38. A. Gupta and K. S. Gandhi, unpublished work.
39. K. K. Agarwal, A. Kumar, D. Kunzru, and S. K. Gupta, *J. Appl. Polym. Sci.*, submitted.

Received January 8, 1982

Accepted February 5, 1982